Appl. Phys. 3, 299—305 (1974)

Applied Physics

Hydrostatic Pressure-Forced Phase Transition from Ferroelectric to Antiferroelectric in Compositions of the $PbZr_{1-x}Ti_xO_3 + 0.8\%\ WO_3$ Type

Paul Gonnard*, François Bauer**, Michel Troccaz*, Yves Fetiveau*, and Lucien Eyraud*

Received 17 July 1973 / Revised 12 December 1973

Abstract. Hydrostatic pressure acting on doped lead titanate-zirconate materials with a considerable proportion of zirconium induces a phase transition between ferroelectric and antiferroelectric states, which causes the previously poled specimens to depolarize. Measurements using a capacitance and those made on short-circuited specimens allow us to draw phase diagrams of the following types: "pressure-electric field" and "pressure-composition". A thermodynamic investigation of the phenomenon permits us to define new characteristic coefficients for this type of depolarization.

Index Headings: Phase transition – Ferro- and antiferro-electricity

Solid solutions suitable for irreversible conversion from mechanical to electric energy take advantage of an hydrostatic-pressure enforced transition from ferroelectric to antiferroelectric (F → AF).

The diagram in Fig. 1 shows the following transitions for increasing temperature:

(a) and (c) $AF_A \rightarrow F_B$, $AF_A \rightarrow AF_B$, $F_A \rightarrow F_B$ } determined from DTA and permittivity plots.

(b) $AF_B \rightarrow F_B$, $AF_A \rightarrow F_A$ } (dotted line) determined from hysteresis loops at low frequency [1].

In the case of x approaching 0.05 – 0.07 the F and AF states are fairly close at room temperature.

It should be born in mind that for all compositions of the perovskite type [2]: the electric field acts to extend the range of stability of the ferroelectric state; and the compressive stress acts to extend the range of stability of the antiferroelectric state.

In the case of a transition occurring between ferroelectric and antiferroelectric states the most important and most easily noticeable modification is

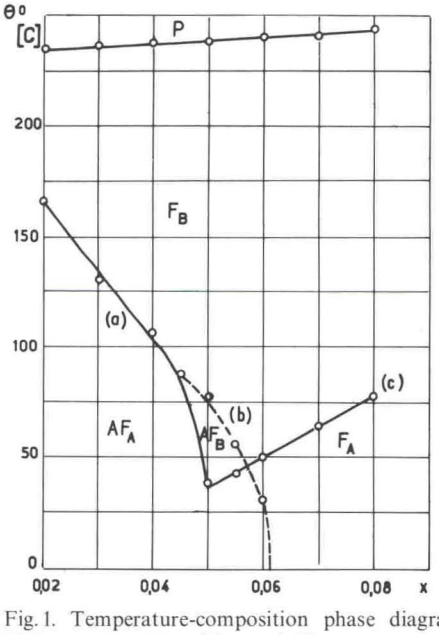

Fig. 1. Temperature-composition phase diagram for $PbZr_{1-x}Ti_xO_3 + 0.8\%\ WO_3$ with x variable, temperature increasing

* Laboratoire de Ferroelectricité Département de Genie Electrique Institut National des Sciences Appliquées, F-69621 Villeurbanne, France.

** Institut Franco-Allemand de Recherches de Saint-Louis, F-68300 Saint-Louis, France.

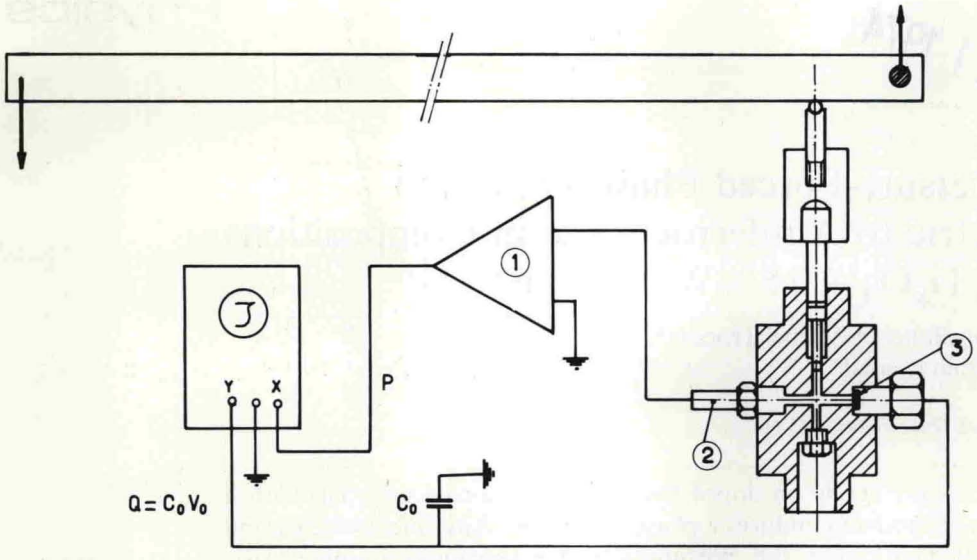

Fig. 2. Schematic diagram of the experimental arrangement, *1* charge amplifier, *2* pressure transducer, *3* ferroelectric ceramic specimen

the loss in remanent polarization of poled specimens [3].

1. Experimental Methods

Experimental Arrangement

Figure 2 exhibits the experimental arrangement used to induce a hydrostatic compression of the ferroelectric ceramics under investigation. The principle of the device is straightforward: a leverarm acts on the primary piston of a high-pressure chamber and allows to reach hydrostatic pressures of the order of 6 – 7 kbar [4].

Measurements Made on Short-Circuited Specimens (Fig. 3)

A capacitor (1300 μF) is connected to the terminals of the specimen. The Voltage V_0 measured by an oscillograph or a high input-impedance recorder does not exceed a few millivolts. The very high time constant given by the capacitor and the impedance of the measuring apparatus allows either isothermal cycles or "quasi-adiabatic" cycles to be performed within a few hundreds of msec. The cycle is drawn by recording the voltage at the terminals of the capacitance as a function of the pressure. This cycle allows to determine the transition pressure as well as the charges liberated from the ceramic.

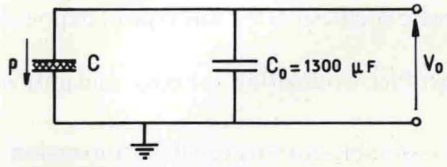

Fig. 3. Measurement circuit

Measurements Made on High Impedance Capacitive Load

A capacitance C_1 of good quality and low value (200 up to 4000 pF) is connected to the terminals of the ceramic. The capacitance C_0 (1300 μF) connected in series within the circuit allows to determine the charge transfers as well as the value of the potential difference at the terminals of the specimen, i.e.

$$V = V_0 \frac{C_0 + C_1}{C_1} \approx V_0 \frac{C_0}{C_1}.$$

Preparation of the Specimens

The specimens (diameter: 5 mm, thickness: 1 mm) are covered with a conducting varnish and poled at room temperature under the influence of a 4000 V/mm field. The specimens containing less than 5% titanium are poled when hot (100° C), they cooled under the influence of the field.

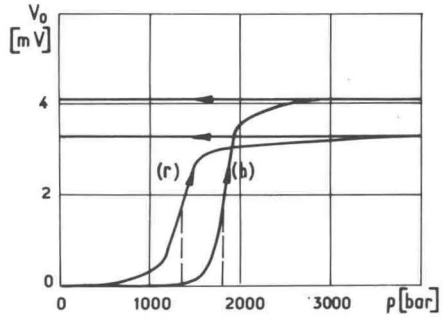

Fig. 4. Charge-pressure cycle $PbZr_{0.95}Ti_{0.05}O_3 + 0.8\%\ WO_3$, *r* poled at room temperature, *h* poled when hot

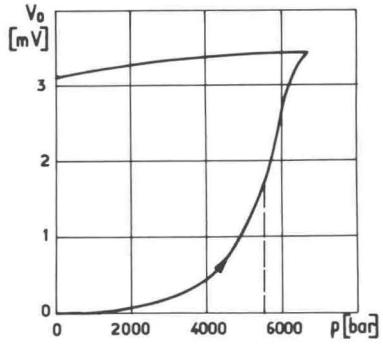

Fig. 6. "Charge-pressure" cycle for $PbZr_{0.92}Ti_{0.08} + 0.8\%\ WO_3$

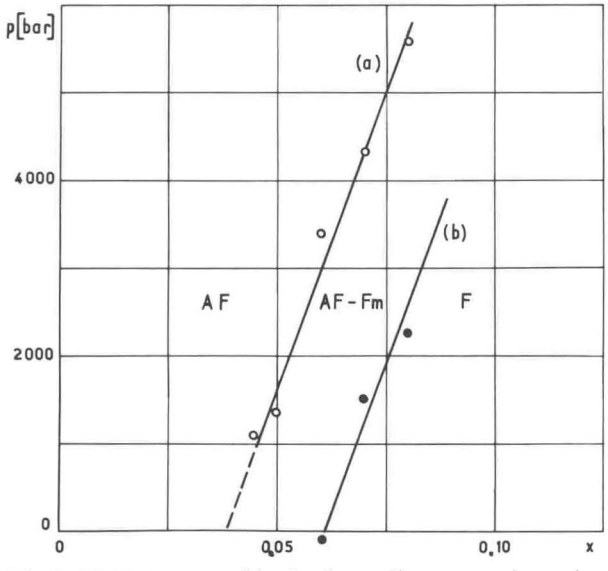

Fig. 5. "Pressure-composition" phase diagram *a* increasing pressure, *b* decreasing pressure

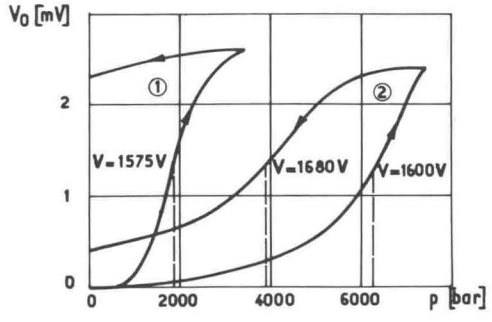

Fig. 7. "Charge pressure-cycle" ($C_1 = 1085$ pF, $C_0 = 1300$ µF) for *1* $PbZr_{0.95}Ti_{0.05}O_3 + 0.8\%\ WO_3$ and *2* $PbZr_{0.92}Ti_{0.08} + 0.8\%\ WO_3$

2. Experimental Results

Depolarization of the Short-Circuited Specimens

The curves *r* and *h* plotted in Fig. 4 show the variation of the "charge pressure" cycles for $x = 0.05$ after polarization of the ceramic when cold and hot, respectively.

This composition is antiferroelectric at room temperature. It becomes metastable ferroelectric (*Fm*), however, if an electric field is applied [5]. Both the low value of the transition pressure and the poor polarizability of the specimen when cold can be explained by the metastable phase. The transition pressure is defined as the abscissa value of the point of the curve whose ordinate value is the half of the charges liberated during the transition process. Preference has, therefore, to be given to the polarization of the specimen when hot, because the F→AF pressure enforced transition is more pronounced and the loss of polarization is increased (approaching the remanent polarization of the material). Analogous results are achieved with compositions of the $x > 0.06$ type for samples polarized when hot or cold. From Fig. 5a and 6 it can be seen that the transition pressure increases rapidly with increasing titanium contents, whereas the charges are liberated in a somewhat less pronounced manner.

Depolarization on Capacitive Loads

In the case of decreasing load capacities, the electric field increases more and more rapidly with the liberated charge. Curve *1* of Fig. 7 illustrates a "charge pressure" cycle for an antiferroelectric composition at room temperature. The transition process occurs over a larger pressure range and the value of the

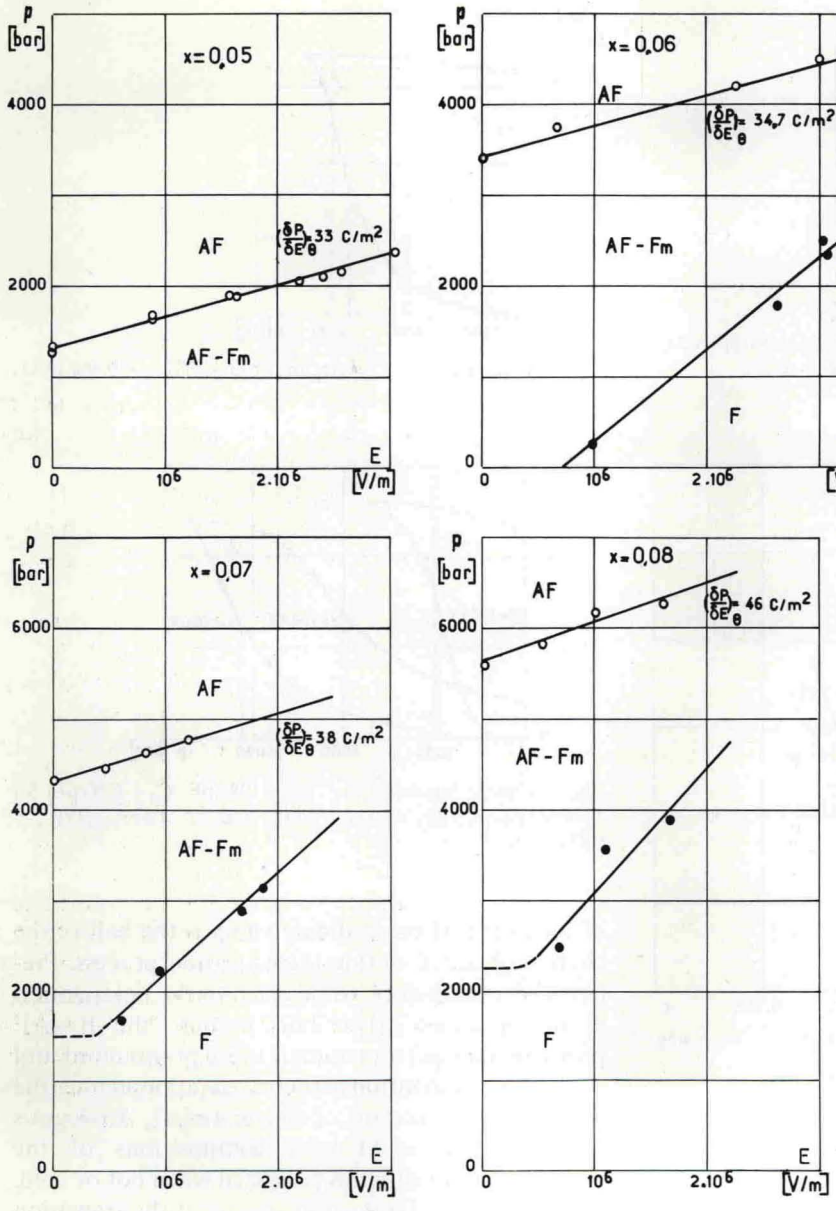

Fig. 8. "Pressure-electric field" phase diagram for various composition (○: increasing pressure, and ●: decreasing pressure)

transition pressure, as defined above, is increased. Finally, a slight repolarization can be observed in the decompression process for strong electric fields.

For ferroelectric compositions at room temperature, the AF→F transition results in a very marked repolarization of the ceramic (Curve 2, Fig. 7). This repolarization is stopped, however, when the value of the electric field falls below that of the coercive field. The transition pressure AF→F in the decompression phase is defined as the abscissa value of that point of the curve whose ordinate is the half the charges recovered by the ceramic.

The electric field corresponding to each transition pressure is given by

$$E=\frac{V}{s} \quad \text{and} \quad V=V_0\,\frac{C_0}{C_1},$$

where s is the thickness of the specimen. In changing the values of the load capacity, it is possible to plot the phase diagram (Fig. 8) "transition pressure electric

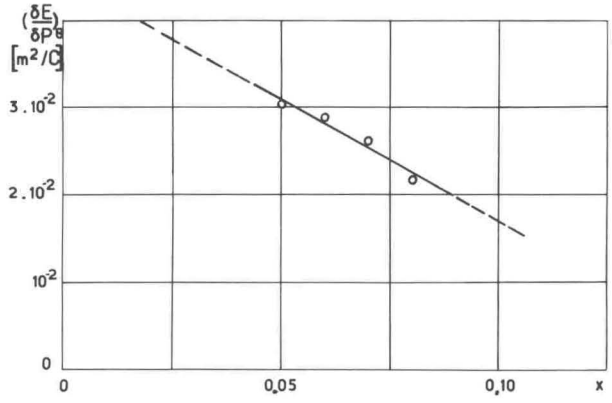

Fig. 9. Variation of $(dE/dP)_0$ versus x

field" for each composition subjected to both the compression and decompression phase. These diagrams confirm that composition with $x = 0.05$ and $x = 0.06$ are antiferroelectric and metastable ferroelectric after polarization.

The compositions corresponding to $x > 0.06$ are ferroelectric since the two transitions F→AF and AF→F, in the absence of action of the electric field, call for a positive pressure.

The transition pressure varies linearly with the electric field. The transition slope F→AF, at increasing pressure, allows $(\delta E/\delta p)_0$ to be determined for this transition (Fig. 9).

The influence of pressure and composition on the F→AF transition is given in Fig. 5. In extrapolating the straight lines $p = f(E)$ representing the AF→F transition in the "pressure-electric field" diagrams, it is possible to derive the pressure of the AF→F transition in the coercive field for each composition (Fig. 8). The transition pressure is assumed to remain constant for values of the electric field that are below those of the coercive field. One obtains the entire phase diagram "pressure-composition" shown in Fig. 5.

3. Thermodynamics of the Pressure Enforced F→AF Transition and Introduction of New Piezoelectric Coefficients

Neglecting any variation in temperature the general equations can be written with only two thermodynamic variables: the electric field E[V/m] and the hydrostatic stress p[N/m²] (p is considered positive for compression). The standard piezoelectric equations $dD = \varepsilon dE - d_h\, dp$ and $dV/V = -S dp + d_h \cdot dE$ can be applied to poled ferroelectrics, metastable or not, only in the case of linear and reversible phenomena. The following symbols are used

dD = variation of dielectric displacement [C/m²],
dV/V = relative volume variation (dimensionless),
S = elastic compliance at constant electric field [m²/N],
$d_h = -(\delta D/\delta p)_E$ = hydrostatic piezoelectric coefficient at constant electric field [C/N],
$\varepsilon = (\delta D/\delta E)_p$ = dielectric permittivity at constant pressure [F/m].

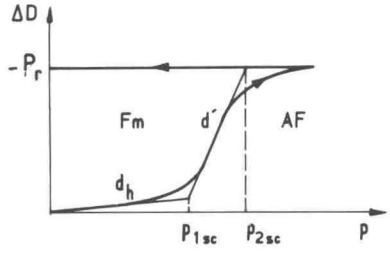

Fig. 10

These relations are valid if the pressure is lower than the pressure p_1 for which the transition takes place. During the transition process, i.e. between the pressures p_1 and p_2 (p_2 = pressure at the end of the transition), it is possible to define three new coefficients d', ε', g' caracterizing the F→AF phase transition. The piezoelectric coefficients $d' = -(\delta D/\delta p)_E$ is the slope of the linear ferroelectric-antiferroelectric phase boundary in the diagram "short circuit charges versus hydrostatic stress" (Fig. 10). The total change of dielectric displacement during the compression results from the liberation of the remanent charge of polarization P_r. From the following equations

$$D = \int_0^D dD = -d' \int_{p_{1sc}}^{p_{2sc}} dp = -P_r$$

and

$$p_{2sc} - p_{1sc} = \Delta p_{sc} = \frac{P_r}{d'}$$

we find easily

$$d' = \frac{P_r}{\Delta p_{sc}}.$$

The permittivity ε' at constant pressure during the transition, i.e. $\varepsilon' = (\delta D/\delta E)_p$, may be defined from the hysteresis loop $P = f(E)$ of samples previously in the

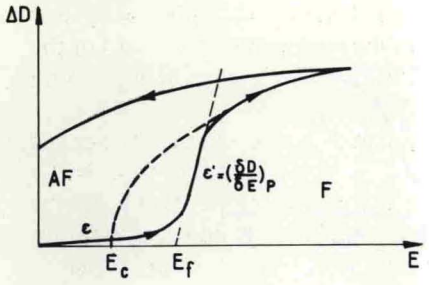

Fig. 11

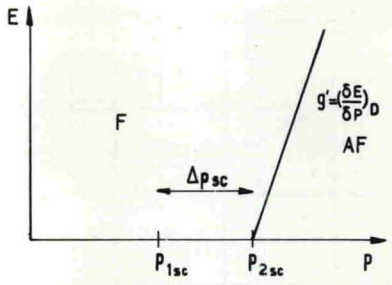

Fig. 12

antiferroelectric state [1]. The quantity ε' denotes the slope of the linear AF→F phase boundary in the diagram "charge density versus electric field" (for the first cycle), see Fig. 11. We assume that ε' has the same value for an F→AF transition.

The piezoelectric coefficient $g' = (\delta E/\delta p)_D$ may be derived by equations similar to the standard piezoelectric equations with new parameters defined for the F→AF transition, namely

$$dD' = \varepsilon' dE - d' dp \tag{1}$$

$$dV'/V = -S' dp + d' dE \tag{2}$$

$$d' = (1/V)(\delta V'/\delta E)_p \quad \text{and} \quad -S' = (1/V)(\delta V'/\delta p)_E ,$$

where S' is the slope of the F→AF phase boundary in the diagram "volume strain versus hydrostatic pressure". From (1) it follows $(\delta E/\delta p)_D = d'/\varepsilon'$. at constant dielectric displacement. For the entire transition taking into account the relative volume change $\Delta V'/V$ and the change of the electric field $\Delta E = P_r/\varepsilon'$ it results the piezoelectric coefficient $d' = (\Delta V'/V)/(P_r/\varepsilon') = \varepsilon' g'$, where $g' = (\Delta V'/V)/P_r = d'/\varepsilon'$.

As a final result we find the same relation as for the standard piezoelectric coefficients g_h and d_h, namely $g_h = d_h/\varepsilon$. We also have

$$-S' = (1/V)(\delta V'/\delta p)_E = -(\Delta V'/V)/\Delta p_{sc}$$
$$= -(\Delta V'/V)/(P_r/d')$$
$$S' = d'g'$$

and (2) becomes $dV'/V = -d'g'dp + d'dE = g'dD'$.

We may remark that in the standard piezoelectric equations the electromechanical coupling factor k is given by $k^2 = d_h g_h/S$. During the transition process the electromechanical factor k is equal to unity: $k'^2 = d'g'/S = 1$. This result, previously mentioned [6], is also obtained by setting the Gibbs free energy equal for states AF and F, i.e.

$$\Delta E \cdot \Delta D' = (\Delta V'/V)\Delta p .$$

This relation shows that the mechanical and electrical energies exchanged during the phase transition are perfectly coupled.

The coefficient g' denotes the slope of the F→AF linear phase boundary in the phase diagram: "electric field versus hydrostatic pressure" (Fig. 12).

(1) and (2) describe only the variations which occur during the phase transition. These changes must be added to the standard piezoelectric effect between p_1 and p_2. So, for each state of the ceramic we have the following equations

Ferroelectric phase

$$p < p_1 \quad \left| \begin{array}{l} dD = \varepsilon dE - d_h dp \\ dV/V = d_h dE - S dp \end{array} \right.$$

During the phase transition:

$$p_1 < p < p_2 \quad \left| \begin{array}{l} dD = \varepsilon dE - d_h dp + \varepsilon' dE - d' dp \\ dV/V = d_h dE - S dp + d' dE - d' g' dp \end{array} \right.$$

Antiferroelectric phase:

$$p > p_2 \quad \left| \begin{array}{l} dD = \varepsilon dE \\ dV/V = -S dp . \end{array} \right.$$

Let us consider now the particular case of an hydrostatic stress applied to an open-circuit ceramic:

For $p < p_1$ we find $dD = 0$ and therefore $dE/dp = d_h/\varepsilon = g_h$ and in the region $p_1 < p < p_2$ for $dD = 0$ we obtain $dE/dp = d'/\varepsilon' = g'$.

Assuming that we have again $\varepsilon dE - d_h d_p = 0$ we note that $dD' = \varepsilon' dE - d' dp = 0$ involves $dV'/V = g' dD' = 0$. The F→AF phase transition is completely clamped by the electric field. The deformation $dV/V = -S dp + d_h dE$ is only due to the standard piezoelectric effect. Near pressure p_1 there is no transition effect, and we have $g_h = g' = d_h/\varepsilon = d'/\varepsilon'$. Therefore the slope of the F→AF linear phase boundary in the diagram "electric field versus hydrostatic pressure" is equal to the standard piezoelectric coefficient g_h.

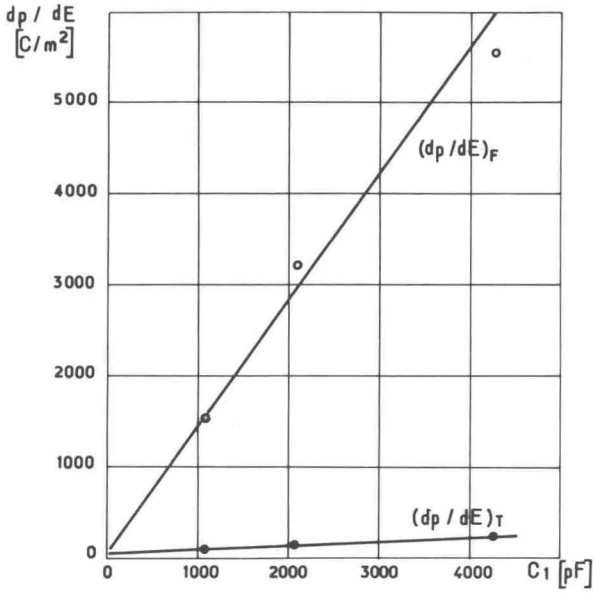

Fig. 13. Variation of $(dP/dE)_F$ and $(dP/dE)_T$ versus ε_1

In the depolarization cycles with capacitive loads the load capacity C_1 can be considered as a ceramic which has the same area A and the same thickness s, as the sample but a permittivity ε_1 such as $C_1 = \varepsilon_1 A/s$. The variation of the dielectric displacement is now a linear function of the electric field: $dD = -\varepsilon_1 dE$ and for pressures lower than p_1 pressure we have $dD = -\varepsilon_1 dE = \varepsilon dE - d_h dp$ and consequently $dp/dE = (\varepsilon + \varepsilon_1)/d_h = 1/g_h + \varepsilon_1/d_h$.

The linear variation of dp/dE versus ε_1 gives the values of d_h and g_h.

Between the pressures p_1 and p_2 we can write $dD = -\varepsilon_1 dE = \varepsilon' dE - d' dp + \varepsilon dE - d_h dp$; *or* $dp/dE = (\varepsilon + \varepsilon' + \varepsilon_1)/(d' + d_h) = (\varepsilon + \varepsilon')/(d_h + d') + \varepsilon_1/(d_h + d') \approx 1/g' + \varepsilon_1/d'$ ($\varepsilon \ll \varepsilon'$, and $d_h \ll d'$).

The dp/dE versus ε_1 relationship is linear and enables us to determine the values of g' and d'. The preceding theoretical considerations are now applied to a sample with $x = 0.08$ and compared with some experimental results.

The nearly linear variations of $(dp/dE)_F$ in the ferroelectric state and $(dp/dE)_T$ during the transition process, as functions of ε_1, are shown in Fig. 13. The g_h value is extrapolated for $\varepsilon_1 = 0$ with a very low precision, because of the important slope $(1/d_h)$ of the curve. Nevertheless, we have $g_h \approx g'$ and $d_h = 61 \times 10^{-12}$ C/N.

From measurements with a capacitance bridge we obtain $\varepsilon = 2.75 \times 10^{-9}$ F/m which leads to $g_h = d_h/\varepsilon = 45^{-1}$ m²/C. The very low slope $(1/d')$ of the $(dp/dE)_T$ curve does not allow a good determination of d'; on the other hand, the g' value is easily obtained to $g' = 43^{-1}$ m²/C and therefore $g_h \approx g'$. For a sample, with $x = 0.07$ the g' and g_h values are

$d_h = 48 \times 10^{-12}$ C/N

$\varepsilon = 2.4 \times 10^{-9}$ F/m $g_h = 50^{-1}$ m²/C $g' = 40^{-1}$ m²/C.

Conclusion

By introduction of two new piezoelectric coefficients d' and g' the behaviour of the materials through a F→AF pressure – enforced phase transition can be explained. We find that d' is much larger than d_h but that g' is quite the same as g_h. These two coefficients have important values for solid solutions having highly coupled dipoles and therefore high remanent polarizations and low permittivities.

Among the various materials which hold such properties, those mentioned in this paper are particularly interesting for irreversible conversion of mechanical to electrical energy (energy storage). By irreversible depolarization of materials previously poled, induced by hydrostatic compression, it is possible to obtain 3 J/cm³ on an resistive load.

References

1. J. Paletto, M. Troccaz, P. Gonnard, G. Grange, L. Eyraud: C.R. Acad. Sc. Paris, t. 275 (30 Oct. 1972), Série B–657
2. D. Berlincourt: IEEE Trans. Sonics Ultrasonics. SU–**15**, 89 (1968)
3. D. Berlincourt, H. H. A. Krueger, B. Jaffe: J. Phys. Chem. Solids **25**, 659 (1964)
4. F. Bauer: Thèse, Lyon (1971)
5. M. Troccaz, J. Perrigot, P. Gonnard, Y. Fetiveau, L. Eyraud: C.R. Acad. Sc. Paris, t 275 (16 Oct. 1972), Série B–597
6. D. Berlincourt: IEEE Trans. Sonics Ultrasonics SU–**13**, 116 (1966)